DOI: 10.1002/ejic.200800750

Di- or Trinuclear 3d–4f Schiff Base Complexes: The Role of Anions

Jean-Pierre Costes,*[a] Bruno Donnadieu,[a][‡] Ruxandra Gheorghe,[a][‡‡] Ghenadie Novitchi,[b] Jean-Pierre Tuchagues,[a] and Laure Vendier[a]

Keywords: Anions / Schiff bases / Transition metals / Lanthanides / Heterometallic complexes

We demonstrate through structural, spectroscopic, and magnetic studies that the main factors governing the nuclearity of M–Gd (M = Cu, Ni) complexes derived from compartmental Schiff base ligands are the different affinities of the lanthanide ions for the potential ligands and anions present in the reaction medium. In the eight examples studied, there is competition between the tetradentate O_2O_2 coordination site of the polydentate ligand and the anionic entities brought by the gadolinium salts. The strong affinity of nitrato anions for lanthanides yields dinuclear complexes and prevents formation of trinuclear entities, whereas the use of poorly coordinating anions such as triflates may yield either dinuclear or trinuclear complexes, depending on the 3d/4f ratio.

Introduction

Bicompartmental Schiff base ligands differing by the nature and size of their coordinating sites (N_2O_2 and O_2O_2) have been of great interest for the synthesis of strictly heterodinuclear 3d–4f complexes and for studying 3d–4f magnetic interactions.[1–3] Because the lanthanide ion is devoid of any orbital contribution, the interaction of copper with gadolinium was studied first.[4–7] Moreover, as such Schiff base ligands are able to chelate several different 3d ions, other couples are accessible.[8] Because these dinuclear entities are well isolated from each other, they are good candidates for studying the unique magnetic interaction that can be active in such complexes, and ferromagnetic interactions have been evidenced in a large majority of heterodinuclear Ni^{II}–Gd,[9] Co^{II}–Gd,[10] Fe^{II}–Gd,[11] and VO–Gd[12] complexes. Few literature reports indicate that di- or trinuclear 3d–4f complexes may be isolated by using a 3d complex as a ligand.[2,13–16] In order to gain a more precise view of such possibilities and a better understanding of the synthetic pathways, we searched for the parameters that may influence the nuclearity of the isolated complexes. Particular attention was paid to the possible role of anions present during the synthesis. They may be considered as auxiliary ligands in comparison to the main Schiff base ligand that chelates the 3d and 4f ions, respectively, in a stepwise process. Furthermore, it was reported that most Cu–Gd complexes having a ferromagnetic interaction are characterized by C_{2v} symmetry,[17] whereas the only complexes exhibiting an antiferromagnetic interaction are of lower symmetry.[18] In order to check the possible role of symmetry, it may thus be of interest to isolate and study complexes of symmetry lower than C_{2v}. This contribution is focused on a series of M–Gd complexes with copper and nickel ions for which the magnetic interactions can be studied by using isotropic spin Hamiltonians. Seven among the eight 3d–4f compounds presented in this contribution are novel.

[a] Laboratoire de Chimie de Coordination du CNRS, UPR 8241, liée par conventions à l'Université Paul Sabatier et à l'Institut National Polytechnique de Toulouse,
205 route de Narbonne, 31077 Toulouse Cedex, France
Fax: +33-5-61553003
E-mail: costes@lcc-toulouse.fr
[b] Institute of Chemistry, Academy of Sciences of Moldova, Academiei str. 3, 2028 Chisinau, Moldova
[‡] Present address: Department of Chemistry, University of California at Riverside,
Riverside, CA 92521, USA
[‡‡] Present address: University of Bucharest, Faculty of Chemistry, Inorganic Chemistry Laboratory,
Str. Dumbrava Rosie nr. 23, 020464 Bucharest, Romania

Supporting information for this article is available on the WWW under http://www.eurjic.org or from the author.

Results and Discussion

Preparation

The 3d-Gd complexes (3d = Cu, Ni) described in the present work were prepared according to the building block approach by using 3d Schiff base complexes as ligands able to yield the expected heteronuclear complexes upon reaction with Gd ions. In the case of copper, two Schiff base complexes $L^1Cu\cdot(H_2O)$ and $L^2Cu\cdot(H_2O)$ were used to yield the 1:1 complexes $L^1CuGd(trif)_3(H_2O)_2$ (**1**) and $[L^2CuGd(trif)_2(H_2O)_2]\cdot(trif)\cdot H_2O\cdot$acetone (**2**) and the 2:1 complex $[(L^1Cu)_2Gd(trif)_2](trif)$ (**3**) by reaction with gadolinium triflate, depending on the Cu/Gd ratio. The molecular structure was determined for one complex of each nuclearity.

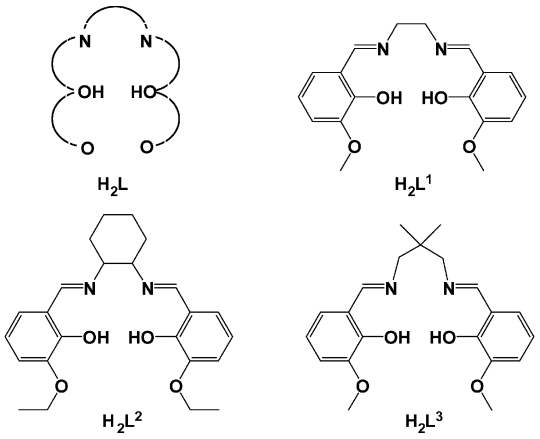

Reaction of $[L^3Ni]\cdot 1.75H_2O$ (**4**) with lanthanide nitrate salts in a 1:1 ratio in acetone yielded the expected complex $[L^3NiGd(NO_3)_3(H_2O)_2]$ (**6**)[9] as a light-purple powder, whereas the same reaction in a 2:1 Ni/Ln ratio produced a beige precipitate formulated as $(L^3Ni)_2Gd(NO_3)_3(H_2O)_2$ (**7**). The latter compound can also be obtained from the reaction of **6** with **4** in a 1:1 ratio in acetone. Further reaction of **6** with sodium dicyanamide in methanol allowed partial removal of the nitrato anions for the resulting complex analyses as $L^3NiGd(N_3C_2)_2(NO_3)$ (**8**). Sodium dicyanamide can also react with **4** to yield $L^3NiNa(N_3C_2)$ (**5**). Use of lanthanide triflate in a 1:1 ratio yielded a practically colorless solution, which, upon addition of dichloromethane, produced an off-white precipitate of $L^3NiGd(trif)_3(H_2O)_2$ (**9**). Unfortunately, we were not able to isolate crystals corresponding to the 2:1 Ni/Gd ratio by using either gadolinium nitrate (complex **7**) or gadolinium triflate. Nevertheless, crystals were isolated for the equivalent europium complex $[\{L^3Ni(H_2O)\}_2Eu(H_2O)](trif)_3$ (**10**).

Infrared, FAB Data, and Electronic Spectra

The formulation of the different complexes resulting from reaction with gadolinium salts is further supported by mass spectrometry (FAB+). Indeed, the spectra of compounds **1**, **2**, and **9** display the most intense signals at *m*/*z* = 845, 899, and 882, which are respectively attributable to $[L^1CuGd(trif)_2]^+$, $[L^2CuGd(trif)_2]^+$, and $[L^3NiGd(trif)_2]^+$ cations. The isotopic patterns, which are perfectly consistent with the attributions, confirm the expected 1:1 Cu/Gd or Ni/Gd ratio. For compound **3**, the main signal corresponds again to $[L^1CuGd(trif)_2]^+$ (100) but two additional signals appearing at *m*/*z* = 1236 (15) $[(L^1Cu)_2Gd(trif)_2]^+$ and *m*/*z* = 1085 (10) $[(L^1Cu)_2Gd(trif)]^+$ are in agreement with the existence of 2:1 Cu/Gd complex **3**. Similar observations were made with nickel complexes **6** and **7**. In these two samples, the main signal corresponds to the $[L^3NiGd(NO_3)_2]^+$ cation, whereas the peaks at *m*/*z* = 1136 (11) $[(L^3Ni)_2Gd(NO_3)_2]^+$ and *m*/*z* = 1072 (9) $[(L^3Ni)_2Gd(NO_3)]^+$ agree with the 2:1 Ni/Gd ratio for **7**. Compound **8**, with two different anions, is characterized by a main peak at *m*/*z* = 712 $[L^3NiGd(C_2N_3)(NO_3)]^+$, which confirms that the nitrato ion is involved in the coordination sphere of gadolinium. Complex **10** behaves as complex **7**, with main signals at *m*/*z* = 877 (100) $[L^3NiEu(trif)_2]^+$ and other signals at *m*/*z* = 1303 (19) $[(L^3Ni)_2Eu(trif)_2]^+$ and *m*/*z* = 1154 (16) $[(L^3Ni)_2Eu(trif)]^+$.

The FAB+ data of copper and nickel complexes **3** and **7** agree with the isolation of well-defined 2:1 M/Gd complexes. If there is no ambiguity for **3**, as confirmed by its X-ray structural determination, the situation is more puzzling for **7**. Indeed, infrared absorptions attributable to L^3Ni and $L^3NiGd(NO_3)_3(H_2O)_2$ entities are present for complex **7**. The decrease in the stretching frequency of the O–H bond with a decrease in the number of water molecules seems to indicate that hydrogen bonds are active. This is corroborated by the color of complex **7** and its magnetic behavior, which is similar to that of a dinuclear Ni–Gd entity.

Additional information can be deduced from the infrared spectra.[19] The OH stretching vibrations of water molecules present in complex **6**, for which we know that the water molecules are bonded to the nickel ion,[9] give two strong bands at 3513 and 3430 cm^{-1}. Broad bands centered at 3500 and 3408 cm^{-1} characterize complex **4**. The structural determination of **4** (see below) shows that water is not coordinated to the nickel ion. These bands are absent in complex **8** containing dicyanamide. Three sharp bands corresponding to ν(CN), ν(CO), and ν(CC) of the ligand at around 1644, 1629 and 1608 cm^{-1} are present in complexes **6** and **8** with a 1:1 Ni/Gd ratio, with additional ν(CN) bands coming from dicyanamide around 2200 cm^{-1} for **8**; only one band is observed for **7**. The N–O asymmetric (1473, 1470 cm^{-1}) and symmetric (1294, 1290 cm^{-1}) stretching vibrations of NO_3 are very similar for complexes **6** and **7**. Bands assigned to ionic nitrato anions are not present in **6**, **7**, and **8**. Two C–O stretching vibrations are observed for **4** and **7**, whereas only one is present for **6**. Three bands are attributable to dicyanamide entities in **5**, and five bands characterize complex **8**. Strong bands at 1284, 1221, and 1167 cm^{-1} [ν(S–O) and $\nu_{as}(CF_3)$, $\nu_s(CF_3)$ of the trifluoromethane sulfonate groups] show no significant variations in the 1:1 and 2:1 copper or nickel complexes **1**, **2**, **3**, and **9** and **10**, respectively.

The solid-state electronic spectra confirm that faint-colored nickel complexes **6**, **8**, and **9** are in an octahedral environment, with $[Ni^{II}N_2O_2O'_2]$ chromophores and two water molecules occupying the axial positions.[20] For example, the UV/Vis spectrum of complex **9** shows three bands: a large one at around 725 nm corresponding to the $^3A_{2g} \rightarrow {}^3T_{2g}$ electronic transition, a second band with a maximum at 580 nm, which is due to the $^3A_{2g} \rightarrow {}^3T_{1g}(F)$ transition, and a shoulder at approximately 438 nm, which can be ascribed to the $^3A_{2g} \rightarrow {}^3T_{1g}(P)$ transition (assuming the O_h point group). The presence of a large band at around 1100 nm for **4** is in agreement with a tetragonal deformation of the NiN_2O_2 chromophore, whereas the band at 512 nm indicates a square planar environment of the nickel ion. The structural determination of **4** (see below) confirms these observations. Compound **7** possesses bands attribut-

able to nickel centers in octahedral and square planar environments. This observation might indicate that **7** is not a genuine trinuclear species. A mixture of independent L^3Ni and $L^3NiGd(NO_3)_3(H_2O)_2$ complexes in a 1:1 ratio may be viewed, or because the compound seems homogeneous, the free outer O_2O_2 site of the L^3Ni unit may be a host towards the aqua ligand coordinated to the nickel ion of the $L^3NiGd(NO_3)_3(H_2O)_2$ complex. A very similar example was recently published.[21] As for complex **10**, the two bands at 936 and 632 nm differ from those observed for the octahedral complexes. They correspond to a NiN_2O_2O' chromophore with the nickel ions in a square pyramidal environment, as confirmed hereunder by the structural determination of complex **10**. Dark-green complex **5** is characterized by an intense band at 621 nm.

Description of the Structures

The molecular plot of $[L^2CuGd(trif)_2(H_2O)_2]\cdot(trif)\cdot H_2O\cdot$ acetone (**2**) sketched in Figure 1 confirms the dinuclear nature of this structure. The copper and gadolinium ions are triply bridged by the two phenoxido oxygen atoms of the L^2 ligand and two oxygen atoms from a triflato anion. A second triflato anion, which is linked to the Gd ion as a monodentate ligand, experiences a weak contact with the copper ion of a neighboring complex through another oxygen atom of the RSO_3^- group (Figure 2). A similar contact is established by the symmetry-related triflato anion linked to the gadolinium ion of that neighboring entity. The third triflate is hydrogen bonded by its three different oxygen atoms to three water molecules coordinated to two different gadolinium ions. Indeed, each Gd ion is coordinated to two water molecules, as a consequence of the low coordination power of the triflate anions. As a result of the presence of a symmetry-related triflate, two dinuclear Cu–Gd complexes are doubly hydrogen bonded. The net result of these weak interactions is the presence of 1D chains based on two dinuclear Cu–Gd entities, in a head-to-tail arrangement, hydrogen bonded by triflate anions through the water molecules coordinated to the gadolinium ions (Figure 2). The L^2 ligand is practically planar, except for the diaminocyclohexyl ring. The dihedral angle between the (OCuO) and (OGdO) planes is equal to 4.0(1)°, and the gadolinium ions are eight coordinate.

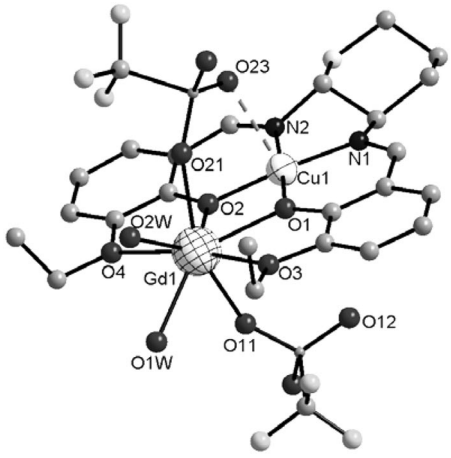

Figure 1. Structure of complex **2** at the 30% probability level. H atoms and the noncoordinated triflate anion are omitted for clarity. Selected bond lengths [Å] and angles [°]: Cu1–N1 1.900(7), Cu1–N2 1.912(7), Cu1–O1 1.903(5), Cu1–O2 1.901(5), Cu1–O23 2.677(7), Gd1–O1 2.299(5), Gd1–O2 2.322(5), Gd1–O11 2.308(5), Gd1–O21 2.382(5), Gd1–O1W 2.425(5), Gd1–O2W 2.376(5), Gd1–O3 2.533(5), Gd1–O4 2.547(5), Cu1–O1–Gd1 106.2(2), Cu1–O2–Gd1 105.4(2), O2–Cu1–O1 82.5(2), O1–Gd1–O2 65.7(2).

One distinctive feature in the structure of **3** is that the trinuclear complex is not neutral but cationic. It corresponds to the formula $[(L^1Cu)_2Gd(trif)_2]^+$. In addition to two trinuclear entities, the unit cell contains two triflate anions. A view of one of the two similar bimetallic cations

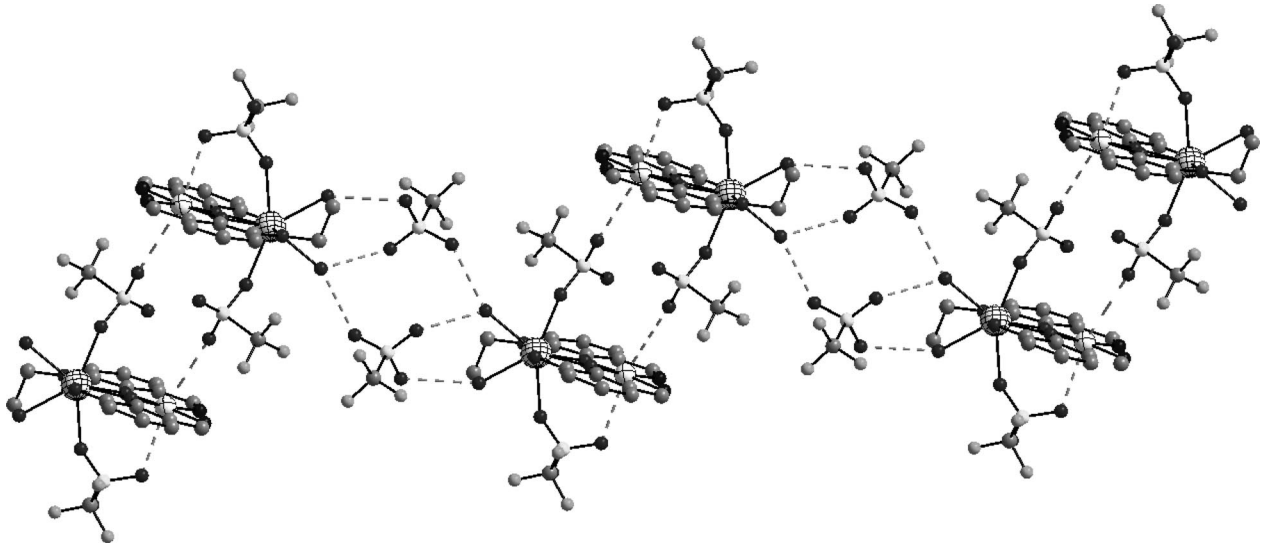

Figure 2. Intermolecular interactions responsible for the supramolecular 1D network in **2**.

is shown in Figure 3 with relevant bond lengths and angles of the Cu^{II} and Gd^{III} environments reported in the figure caption. There is a very small difference between the (L^1Cu)-Gd/2 moieties. Coordination of the gadolinium ion to two L^1Cu entities introduces a slight tetrahedral deformation of the N_2O_2 coordination sites of copper, which implies a λ deformation of the five-membered copper diamino rings. The central gadolinium ion is linked to each copper ion by two phenoxido bridges and by a triflato anion. The copper ion adopts a square-based 4+1 coordination mode, and the equatorial donors are provided by the L^1 ligand and the axial position is occupied by the μ-bridging SO_2 group of the triflato anion. The related Cu···Gd separations are 3.379(1) and 3.384(1) Å. The dihedral angles (*α*) between the (OCuO) and (OGdO) planes are 5.8(1) and 5.0(2)° for the Cu1 and Cu2 moieties, respectively, with an angle of 53.0(2)° between the two OGdO planes. The two OMe side arms of each L^1 ligand are also coordinated to the Gd ion: the gadolinium ion is thus ten-coordinate to four oxygen atoms of each L^1Cu entity and two oxygen atoms from two triflato ligands. As previously noted, the Gd–O bond lengths depend on the nature of the oxygen atoms: the bonds involving the phenoxido [2.346(5)–2.382(4) Å] and triflato [2.393(5) and 2.413(5) Å] oxygen atoms are shorter than those involving the methoxy side arms [2.662(5) and 2.704(5) Å], and two of them are even longer [2.801(5) and 2.957(5) Å] as a consequence of the slight tetrahedral deformations of the copper coordination sphere. Each copper ion is in a usual square-pyramidal environment. The four basal donors (N_2O_2) originate from an L^1 ligand, whereas an oxygen atom of the triflato bridge occupies the apical position. As usual, the apical Cu–O bonds [2.467(6), 2.610(8) Å] are longer than the equatorial ones (mean value: 1.915 Å). Other intermolecular Gd···Cu, Gd···Gd, and Cu···Cu separations are larger than ca. 6.4 Å, whereas the Cu1···Cu2 distance within the trinuclear entity is 6.010(2) Å.

The unit cell of **4** includes two neutral L^3Ni entities, L^3Ni_a and L^3Ni_b, and three and a half unbound water molecules. A view of the L^3Ni_a entity is shown in Figure 4, whereas relevant bond lengths and angles of the Ni^{II} environment of the two L^3Ni species are reported in the figure caption. If the bond lengths do not differ in these two neutral L^3Ni complex molecules, the tetrahedral deformation of the central Ni ion is larger in L^3Ni_a. The six-membered ring formed by the diamino moiety chelating the Ni^{II} ion is in a *δ* twist-boat form in L^3Ni_a (Figure 4). The δ twist-boat conformation is also observed in the L^3Ni_b unit. Because the compound crystallizes in a centrosymmetric space group, it is clear that the enantiomeric λ form is also present in the crystal.

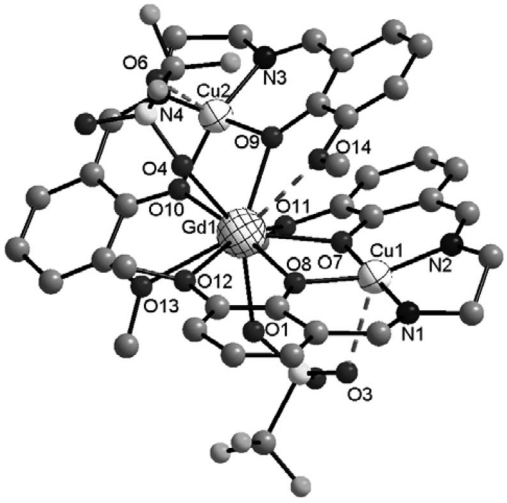

Figure 3. Structure of complex **3** at the 30% probability level. H atoms are omitted for clarity. Selected bond lengths [Å] and angles [°]: N1–Cu1 1.912(6), N2–Cu1 1.933(6), O7–Cu1 1.897(5), O8–Cu1 1.922(5), O2–Cu1 2.563(6), N3–Cu2 1.917(6), N4–Cu2 1.923(6), O9–Cu2 1.920(5), O10–Cu2 1.921(5), O5–Cu2 2.591(6), O1–Gd1 2.413(5), O4–Gd1 2.393(5), O7–Gd1 2.346(5), O8–Gd1 2.377(5), O9–Gd1 2.382(4), O10–Gd1 2.348(5), O11–Gd1 2.801(5), O12–Gd1 2.704(5), O13–Gd1 2.663(5), O14–Gd1 2.957(5), Cu1–Gd1 3.379(1), Cu2–Gd1 3.384(1), Cu1–O7–Gd1 105.3(2), Cu1–O8–Gd1 103.3(2), O7–Cu1–O8 84.8(2), O8–Gd1–O7 66.1(2), Cu2–O9–Gd1 103.0(2), Cu2–O10–Gd1 104.2(2), O9–Cu2–O10 85.6(2), O9–Gd1–O10 67.0(2).

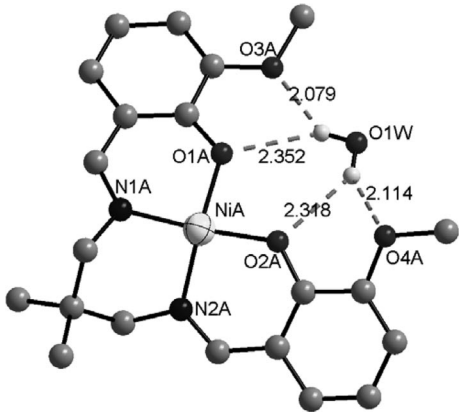

Figure 4. Structure of complex **4** at the 30% probability level. H atoms are omitted for clarity. Selected bond lengths [Å] and angles [°] for the L^3NiA unit: NiA–O2A 1.852(2), NiA–O1A 1.860(2), NiA–N1A 1.862(2), NiA–N2A 1.873(2), O1A–H11W 2.352(5), O3A–H11W 2.079(5), O2A–H12W 2.318(5), O4A–H12W 2.114(5), O2A–NiA–O1A 85.94(8), O2A–NiA–N1A 162.41(9), O1A–NiA–N1A 93.74(9), O2A–NiA–N2A 94.55(9), O1A–NiA–N2A 161.20(9), N1A–NiA–N2A 91.37(10); and for the L^3NiB unit: NiB–O1B 1.857(2), NiB–O2B 1.862(2), NiB–N2B 1.868(2), NiB–N1B 1.877(2), O1B–H31W 2.239(5), O3B–H31W 2.200(5), O2B–H32W 2.426(5), O4B–H32W 2.023(5), O1B–NiB–O2B 85.03(9), O2B–NiB–N1B 169.96(9), O1B–NiB–N1B 92.67(9), O2B–NiB–N2B 93.31(9), O1B–NiB–N2B 170.06(9), N2B–NiB–N1B 90.59(10).

The structural determination of complex **10** evidences a trinuclear cationic Ni–Eu–Ni complex, as shown in Figure 5. The green platelets we isolated were not pure single crystals, so we kept carbon atoms in isotropic thermal motion and we obtained a low-resolution structure with a low value of θ and an elevated value of R_{int}. Nevertheless, X-ray structure determination of **10** confirmed the existence

of a trinuclear Ni–Eu–Ni complex. Comparison with complex **3** highlights several differences. The formula of the cation is $[\{L^3Ni(H_2O)\}_2Eu(H_2O)]^{3+}$. A water molecule is coordinated to each metal ion, whereas the three triflate anions act as counterions. The europium center is nine-coordinate to the four phenoxido and the four methoxy oxygen atoms of the two L^3 ligands and to the water molecule. Surprisingly, the nickel ions are five-coordinate, and they are linked equatorially to the N_2O_2 coordination site of the ligand and axially to a water molecule. Complexation of the lanthanide induces a conformational change in the six-membered diamino ring from a twist-boat to a chair. The L^3Ni moiety is not planar, as it adopts an umbrella shape with the water molecule pointing above the plane. The related Ni···Eu separations are equal to 3.522(3) and 3.534(3) Å. The angle between the two OEuO planes containing the phenoxido oxygen atoms bridging the Ni and Gd ions is 53.0(2)°.

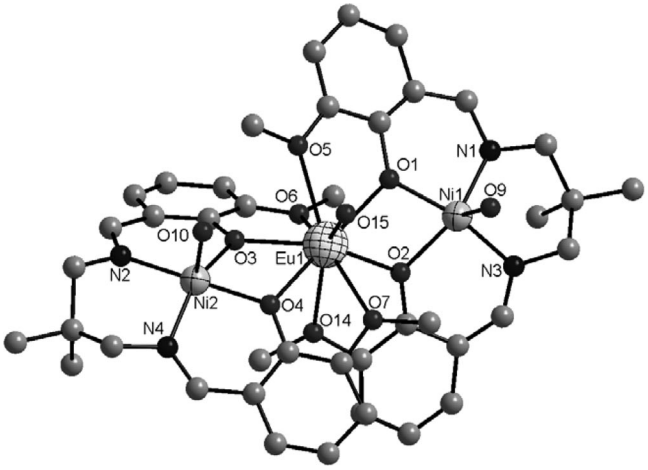

Figure 5. Structure of the $[(L^3NiH_2O)_2Eu(H_2O)]^{3+}$ cation **10** at the 30% probability level. H atoms are omitted for clarity.

Magnetic Data

The magnetic susceptibilities of Cu–Gd complexes **1**, **2**, and **3** were measured in the 2–300 K temperature range with an applied magnetic field of 0.1 T. The thermal variation of the $\chi_M T$ product for complex **1** is shown in Figure 6a, where χ_M is the molar magnetic susceptibility of the dinuclear species corrected for the diamagnetism of the ligands. At 300 K, $\chi_M T$ is equal to 8.25 $cm^3 K mol^{-1}$, which corresponds to the value expected for the two uncoupled metal ions (8.3 $cm^3 K mol^{-1}$). Upon lowering the temperature, $\chi_M T$ increases up to 10.1 $cm^3 K mol^{-1}$ at 5 K. This value compares well with that (10 $cm^3 K mol^{-1}$) expected for an $S = 4$ spin-state resulting from ferromagnetic coupling between Cu^{II} ($S = 1/2$) and Gd^{III} ($S = 7/2$), assuming $g_{Cu} = g_{Gd} = 2.0$. A quantitative analysis was performed on the basis of an expression derived from the spin-only Hamiltonian:[1c]

$$H = -J_{CuGd}S_{Cu}S_{Gd}$$

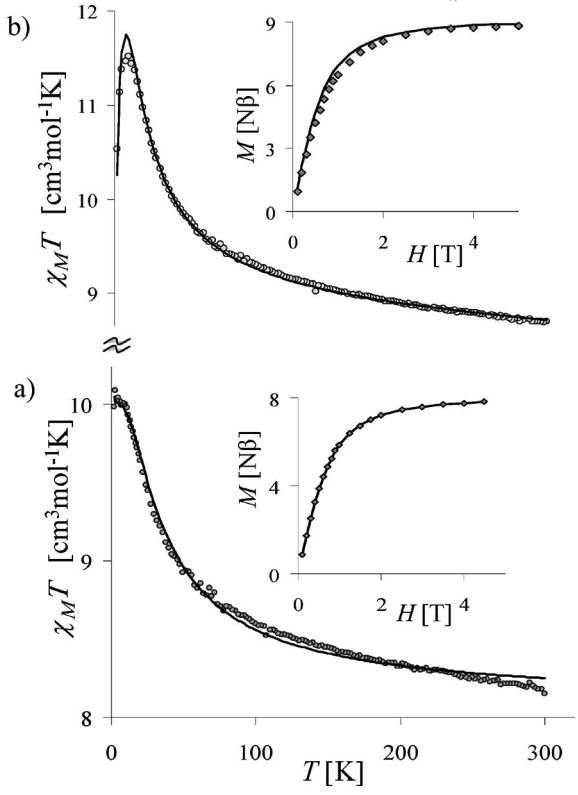

Figure 6. Thermal variation of the $\chi_M T$ product for complexes (a) **1** and (b) **3**. The solid line corresponds to the best-fit data (see text). The inset shows the field dependence of the magnetization for each respective compound.

Least-squares fitting to the experimental data leads to $J_{CuGd} = 8.0(2)$ cm^{-1}, $g_{Cu} = 2.18(2)$, and $g_{Gd} = 1.98(1)$ with a good agreement factor $R = \Sigma(\chi_M T)_{obs} - [(\chi_M T)_{calc}]^2/\Sigma[(\chi_M T)_{obs}]^2$ ($R = 1 \times 10^{-4}$). In order to take into account the constant $\chi_M T$ values at very-low temperatures, a Weiss constant θ of –0.03 K was introduced into the theoretical expression. Complex **2** is characterized by very similar parameter values, $J_{CuGd} = 8.6(2)$ cm^{-1}, $g_{Cu} = 2.2(2)$, $g_{Gd} = 1.98(1)$, $\theta = -0.01$ K, and $R = 1 \times 10^{-4}$ (Figure S1). The temperature-dependent magnetic susceptibility of trinuclear complex **3** was modeled with the expression derived from the isotropic spin Hamiltonian:

$$H = -J_{Cu1Gd}S_{Cu1}S_{Gd} - J_{Cu2Gd}S_{Cu2}S_{Gd} - j_{Cu1Cu2}S_{Cu1}S_{Cu2}$$

Least-squares fitting yields $J_{Cu1Gd} = J_{Cu2Gd} = 5.2(2)$ cm^{-1}, $g = 2.02(2)$, $\theta = -0.45(1)$ K, and $R = 1 \times 10^{-4}$ with $j_{Cu1Cu2} = 0$ (Figure 6b). In these three complexes, the ferromagnetic Cu–Gd interaction is definitely supported by the field dependence of the magnetization M at 2 K. The experimental values are correctly fitted with the Brillouin function for an $S = 4$ spin state (complexes **1** and **2**) and an $S = 9/2$ spin state (complex **3**; see insets of Figure 6).

The room-temperature $\chi_M T$ product of 0.55 $cm^3 mol^{-1} K$ for the $[L^3Ni]\cdot 1.75H_2O$ (**4**) nickel precursor complex is lower than that expected for a paramagnetic high-spin Ni^{II} cation (1 $cm^3 mol^{-1} K$). Indeed, the two L^3Ni conformers present in the solid state have different tetrahedral defor-

$$\chi_M = \frac{N\beta^2}{3k(T-\theta)} \cdot \frac{\frac{495}{2}\cdot g_{\frac{9}{2}}^2 + 126\cdot g_{\frac{7}{2}}^2 \exp\frac{-9J_{NiGd}}{2kT} + \frac{105}{2}\cdot g_{\frac{5}{2}}^2 \exp\frac{-8J_{NiGd}}{kT}}{10 + 8\cdot\exp\frac{-9J_{NiGd}}{2kT} + 6\cdot\exp\frac{-8J_{NiGd}}{kT}}$$

where $g_{\frac{5}{2}} = \frac{-10}{35}g_{Ni} + \frac{45}{35}g_{Gd}$; $g_{\frac{7}{2}} = \frac{4}{63}g_{Ni} + \frac{59}{63}g_{Gd}$; and $g_{\frac{9}{2}} = \frac{2}{9}g_{Ni} + \frac{7}{9}g_{Gd}$

mations, which yield different contributions to the magnetic moment. Surprisingly, the nickel ion in complex **5** with the sodium ion in the outer coordination site of the ligand is low spin and diamagnetic, whereas it is high spin when a gadolinium ion occupies the same location as the sodium ion. Indeed, the $\chi_M T$ value at room temperature (8.80 $cm^3 mol^{-1} K$) for complex **9** corresponds to that expected for noninteracting S = 1 and S = 7/2 ions (8.87 $cm^3 mol^{-1} K$). The thermal dependence of $\chi_M T$ for **9** is shown in Figure 7a. Following a minute increase from 300 to 70 K, the $\chi_M T$ product increases sharply below 70 K and reaches a value of 11.35 $cm^3 K mol^{-1}$ at 2 K. This behavior is reminiscent of the one for the previously published heterodinuclear Ni–Gd complex.[9] The use an exact diagonalization of the E matrix for an S_1 = 1, S_2 = 7/2 dinuclear system with the MAGPACK program and by taking into account a zero-field splitting (zfs) parameter, D, for the nickel ion yields nice agreement between the experimental and calculated values for the parameter values: J_{NiGd} = 2.7 cm^{-1}, D = 12.9 cm^{-1}, and g = 1.99. These data were also fitted with the conventional expression given above and obtained from the Hamiltonian $H = -J_{NiGd}S_{Ni}S_{Gd}$.[9]

In this case, an intermolecular interaction term is considered to account for the zfs of Ni^{II}. The corresponding results are then J_{NiGd} = 2.7(1) cm^{-1}, g = 1.99(1), and θ = –0.36(1) K. For complex **8**, these values are J_{NiGd} = 2.4(1) cm^{-1}, $g_{Gd} = g_{Ni}$ = 2.0(1), and θ = –0.14(1) K (Figure S2). By using the MAGPACK program and by taking into account a D parameter for **8** the following values were obtained: J_{NiGd} = 2.2 cm^{-1}, D = 6.5 cm^{-1}, and g = 1.99.

At first sight, the magnetic behavior of complex **7** is more puzzling. The considered formulation indicates that two nickel and one gadolinium ions are present, whereas the $\chi_M T$ value of 9.08 $cm^3 K mol^{-1}$ at 300 K is similar to that observed for dinuclear complex **9**. Fitting these data as a dinuclear entity yields nice agreement and evidences that one nickel ion does not contribute to the magnetic susceptibility (Figure 7b). The results, J_{NiGd} = 2.5(1) cm^{-1}, D = 10.8 cm^{-1}, and g = 2.01(1), are in complete accordance with those found for complexes **6** and **8**. A fit considering intermolecular interactions yields similar results with J_{NiGd} = 2.4(1) cm^{-1}, $g_{Gd} = g_{Ni}$ = 2.02(1), and θ = –0.25(1) K. The magnetization value of 8.65 Nβ at 5 T (insert of Figure 7b) is in complete agreement with such a behavior.

The magnetic study of complex **10** is trickier due to the orbital contribution of the europium ion. Nevertheless, it confirms that the two nickel ions are clearly in a high-spin state, at variance with complex **7**. The $\chi_M T$ product of complex **10** at room temperature is 4.1 $cm^3 mol^{-1} K$, a value

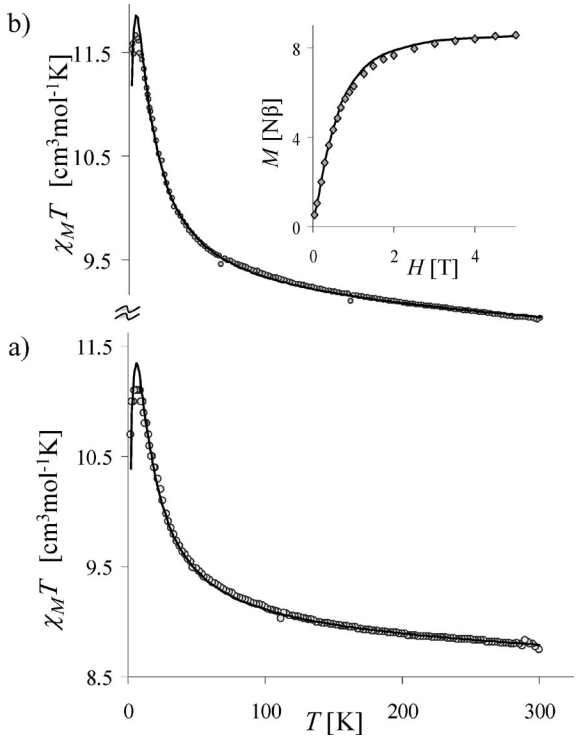

Figure 7. Thermal variation of the $\chi_M T$ product for complexes (a) **9** and (b) **7**. The solid line corresponds to the best-fit data (see text). The inset shows the field dependence of the magnetization for compound **7**.

slightly larger than that expected for two nickel and one europium[22] ions without magnetic interaction (3.74 $cm^3 mol^{-1} K$). The slight $\chi_M T$ decrease followed by a sharp decrease below 50 K is probably the consequence of at least two magnetic phenomena: the depopulation of the Stark levels of the lanthanide ion, along with the zero-field splitting of the nickel ions at very low temperatures (Figure S3).

Discussion

The structural determinations of complexes **2** and **3** clearly demonstrate that the nuclearity of the Cu–Gd complexes prepared with Schiff base compartmental ligands is only a function of the LCu/Gd ratio when poorly coordinating anions such as triflates are used in the presence of a poorly coordinating solvent such as acetone. Indeed, previous X-ray studies of Cu–Ln complexes involving nitrato,[1,9–12] thiocyanato,[23] and diketonato[24] anions or li-

gands have always evidenced heterodinuclear Cu–Ln complexes. Even the chloride anions,[1c] which are not good ligands for lanthanide cations, have yielded dinuclear entities. Until now, only the acetate[2] and trifluoroacetate[13] anions have yielded dinuclear Cu–Ln and trinuclear Cu–Ln-Cu Schiff base complexes. In order to confirm these results, we studied the more intricate case of Ni–Ln complexes. In addition to the change in nuclearity, the ligand field may generate a spin change of the nickel cations. Because only low-spin complexes are formed with Schiff base ligands able to yield a five-membered chelate ring including the nickel(II) ions and the ethylene-bridged diamino moiety, we used 2,2-dimethyl-1,3-diaminopropane as the diamino precursor. We previously showed that the nickel ion is high spin in the $L^3NiGd(NO_3)_3(H_2O)_2$ (**6**) complex,[9] with a ferromagnetic Ni–Gd interaction of 3.6 cm^{-1}, which is the largest found until now in heteronuclear Ni–Gd complexes.[25,26] For a better understanding of the behavior of these nickel complexes, we solved the structure of the precursor complex $[L^3Ni]\cdot 1.75H_2O$ (**4**). The first surprise arose from the observation of uncoordinated water molecules in this nickel complex. Furthermore, there are two L^3Ni molecules in the unit cell, with different tetrahedral deformations. This most probably explains the reduced magnetic moment of **4**, and both $[L^3Ni]$ molecules contribute with a different weight to the magnetic moment. Introducing one gadolinium ion yields complex **6** in which the nickel ions are high spin in an octahedral environment, with two axially coordinated water molecules. Indeed, the $\chi_M T$ value for **6** at room temperature (9.0 $cm^3 mol^{-1} K$) corresponds to what is expected for noninteracting $S = 1$ and $S = 7/2$ ions (8.87 $cm^3 mol^{-1} K$). The behavior of complex **7**, obtained through two different experimental procedures, either by treating **6** with **4** in a 1:1 ratio or by treating **4** with $Gd(NO_3)_3\cdot 5H_2O$ in a 2:1 ratio is more puzzling. The analytical results correspond to the formulation $(L^3Ni)_2Gd(NO_3)_3(H_2O)_2$. The FAB+ data confirm that the main signal corresponds to the $[L^3NiGd(NO_3)_2]^+$ cation (100) and that secondary signals at m/z = 1136 (11) $[(L^3Ni)_2Gd(NO_3)_2]^+$ and m/z = 1072 (9) $[(L^3Ni)_2Gd(NO_3)]^+$ are in agreement with a 2:1 Ni/Gd ratio. At variance with this result, the $\chi_M T$ product at 300 K (9.1 $cm^3 mol^{-1} K$) suggests that one nickel ion is in the high-spin state ($S = 1$), whereas the second nickel ion is low spin ($S = 0$), in accordance with the presence of only two water molecules in the formulation of **7** and the absence of ionic nitrate in its infrared spectrum. It is worth noting that the nickel ion in complex **5**, which is devoid of a water molecule, is also in the low-spin state. Indeed, chelation of three nitrato anions (confirmed by IR spectroscopic data) along with the coordination of four oxygen atoms from L^3Ni prevents coordination of a second L^3Ni unit around the gadolinium ion. Fitting the theoretical expression for a dinuclear Ni–Gd complex to the magnetic data of **7** yields a very nice result (Figure 7b) with a J_{NiGd} value (2.5 cm^{-1}) slightly smaller than that obtained for complex **6**. This result confirms that complex **7** is not a genuine trinuclear Ni–Gd–Ni complex and that the low-spin L^3Ni complex is not directly linked to the gadolinium ion.

The $L^3NiGd(N_3C_2)_2(NO_3)$ complex (**8**) is obtained through partial exchange of the nitrato anions of **6** with dicyanamido anions. The FAB+ data do confirm that the remaining nitrato anion is chelated to the Gd^{III} cation. This complex, analyzed as a dinuclear unit, yields a J_{NiGd} value of 2.2 cm^{-1}, which is very similar to that found for **7**. Very recently, the structural characterization of a novel trinuclear Ni–Pr–Ni complex obtained through a different experimental procedure confirmed the absence of a nitrato anion in the coordination sphere of Pr^{III}.[27] The magnetic study evidences that the two nickel ions of this latter trinuclear complex are high spin, which is in agreement with the observation made for complex **10**. Indeed, the room-temperature $\chi_M T$ product of complex **10** confirms again that the two nickel ions are clearly in the high-spin state. From these observations, we can firmly conclude that the presence of nitrato anions in complex **7** prevents formation of a trinuclear entity. Data dealing with trinuclear Ni–Gd–Ni complexes are scarce,[25,28,29] and there are no examples of a structurally characterized Ni–Gd–Ni complex prepared with H_2L Schiff base ligand (formulae, second page).

Concerning the interpretation of the magnetic data, the meaning of the θ parameter necessary to fit the slight decrease in $\chi_M T$ at very low temperatures is not fully understood. This slight $\chi_M T$ decrease may result from weak interactions between heterodinuclear entities through the hydrogen-bond network or more probably may depend on partial saturation of the large magnetic moment in the magnetic field at low temperature, as previously observed.[1a] In the case of complexes containing nickel ions, it is possible to introduce an axial zero-field splitting parameter D. Surprisingly, the different fits yield rather large D values. A recent review indicates that D values compiled for hexacoordinate nickel compounds span the –22 to +12 cm^{-1} range and that positive D parameters are associated with a weakening of the axial bonds.[30] Although these arguments are subject to debate, it is clear that the J_{NiGd} and g values are well determined by the fitting procedures, whereas the D values are not; then, a general parameter like θ seems to be more appropriate in the present case.

Conclusions

The results presented in this report clearly demonstrate that the high affinity of the lanthanide cations for nitrato anions does not allow trinuclear Cu–Ln-Cu or Ni–Ln-Ni complexes to be prepared from symmetrical Schiff base compartmental ligands if the latter anions are present in solution. Such complexes can be prepared only if the affinity of the lanthanide cations for the anions present in the reaction medium is lower than their affinity for the O_2O_2 coordination site of the 3d ligand complex, L^xCu or L^xNi. Indeed, competition between the main and auxiliary ligands or anions to enter the lanthanide coordination sphere determines the nuclearity of the resulting complex. We must emphasize that the role of solvent has not been taken into account, for these 3d–4f complexes have been prepared by

using acetone, which is a poorly coordinating and dissociating solvent. It is also clear that the ligand field strength is modulated by the coordination of the lanthanide cation in the case of nickel complexes, which thus allows introduction of auxiliary ligands in the axial position of the nickel coordination sphere. At variance, the less positive sodium ion, which yields only 1:1 3d/alkali metal complexes, is not able to produce such a change. Eventually, the seven 3d-Gd complexes considered in the present report display a ferromagnetic interaction between the two metal ions, in consonance with a large majority of the previously reported dinuclear 3d-Gd complexes and, moreover, with fairly large J_{MGd} values. Furthermore, the trinuclear Cu–Gd–Cu entity is a new example of a 3d–4f compound without C_{2v} symmetry that yields ferromagnetic Cu–Gd interactions.

Experimental Section

Materials: The different metal aldimine complexes, $L^1Cu{\cdot}H_2O$,[8] $L^2Cu{\cdot}2H_2O$,[1b] $[L^3NiGd(NO_3)_3(H_2O)_2]$,[9] [$H_2L^1$: *N*,*N*′-ethylenebis(3-methoxysalicylideneimine); H_2L^2: *N*,*N*′-cyclohexanebis(3-ethoxysalicylideneimine); H_2L^3: *N*,*N*′-2,2-dimethylpropylenebis(3-methoxysalicylideneimine)], were prepared as described previously. $Gd(NO_3)_3{\cdot}5H_2O$ and $Gd(CF_3SO_3)_3$ (Aldrich) were used as purchased. High-grade solvents were used for preparing the complexes. The CF_3SO_3 anion is abbreviated "trif" throughout this contribution, whereas C_2N_3 corresponds to the dicyanamide anion.

$L^1CuGd(trif)_3{\cdot}(H_2O)_2$ (1): A mixture of $L^1Cu{\cdot}H_2O$ (0.21 g, 5×10^{-4} mol) and $Gd(trif)_3$ (0.30 g, 5×10^{-4} mol) in acetone (20 mL) was stirred for 30 min and then filtered. Addition of diethyl ether whilst stirring yielded a red precipitate that was filtered off after 30 min and dried. Yield: 0.31 g (60%). IR (KBr): $\tilde{\nu}$ = 3414, 1642, 1608, 1474, 1456, 1442, 1283, 1224, 1175, 1077, 1029, 954, 855, 739, 638, 517 cm^{-1}. MS (FAB+, 3-nitrobenzyl alcohol matrix): *m*/*z* = 845 (100), $[L^1CuGd(trif)_2]^+$. $C_{21}H_{22}CuF_9GdN_2O_{15}S_3$ (1030.40): calcd. C 24.5, H 2.2, N 2.7; found C 24.7, H 2.5, N 2.7.

$[L^2CuGd(trif)_2(H_2O)_2]{\cdot}trif{\cdot}H_2O{\cdot}$acetone (2): The same experimental procedure used with $L^2Cu{\cdot}H_2O$ yielded complex **2** (0.38 g, 65%). IR (KBr): $\tilde{\nu}$ = 3400, 2947, 2867, 1714, 1636, 1608, 1558, 1472, 1393, 1306, 1284, 1223, 1175, 1087, 1029, 991, 888, 749, 637, 575, 517, 428 cm^{-1}. MS (FAB+, 3-nitrobenzyl alcohol matrix): *m*/*z* = 899 (100) $[L^2CuGd(trif)_2]^+$. $C_{30}H_{38}CuF_9GdN_2O_{16}S_3$ (1170.62): calcd. C 30.8, H 3.3, N 2.4; found C 30.5, H 3.2, N 2.3. Slow crystallization of the microcrystalline powder from acetone yielded crystals suitable for X-ray diffraction study.

$[(L^1Cu)_2Gd(trif)_2](trif)$ (3): A mixture of $L^1Cu{\cdot}H_2O$ (0.1 g, 2.5×10^{-4} mol) and $Gd(trif)_3$ (0.075 g, 1.25×10^{-4} mol) in acetone (10 mL) was stirred for 15 min and then filtered. Slow diffusion of diethyl ether into the acetone solution yielded crystals suitable for X-ray diffraction study. The crystals were isolated by filtration and air dried. Yield: 0.12 g (71%). IR (KBr): $\tilde{\nu}$ = 1636, 1609, 1472, 1457, 1443, 1284, 1221, 1167, 1078, 1030, 1028, 953, 857, 739, 637, 516 cm^{-1}. MS (FAB+, 3-nitrobenzyl alcohol matrix): *m*/*z* = 1236 (15) $[(L^1Cu)_2Gd(trif)_2]^+$, 1085 (10) $[(L^1Cu)_2Gd(trif)]^+$, 845 (100) $[L^1CuGd(trif)_2]^+$. $C_{39}H_{36}Cu_2F_9GdN_4O_{17}S_3$ (1384.26): calcd. C 33.8, H 2.6, N 4.0; found C 33.5, H 2.5, N 3.9.

$[L^3Ni]{\cdot}1.75H_2O$ (4): Orthovanillin (1.52 g, 1×10^{-2} mol) and 2,2-dimethyl-1,3diaminopropane (0.51 g, 0.5×10^{-2} mol) were dissolved in ethanol (100 mL), and the solution was stirred for 15 min. Addition of $Ni(Ac)_2{\cdot}4H_2O$ (1.24 g, 0.5×10^{-2} mol) and triethylamine (2.02 g, 2×10^{-2} mol) with stirring yielded a red precipitate that was filtered off after 2 h. The solid was washed with cold ethanol and air dried. Yield: 2.0 g (87%). IR (KBr): $\tilde{\nu}$ = 3502, 2935, 1646, 1612, 1473, 1451, 1319, 1245, 1231, 1082, 1071, 860, 739, 730, 650, 526, 489 cm^{-1}. UV/Vis: λ = 450 (sh.), 512, 628, 1100 nm. $C_{21}H_{27.5}N_2NiO_{5.75}$ (458.65): calcd. C 55.0, H 6.0, N 6.1; found C 54.7, H 6.0, N 6.1. Slow crystallization of the microcrystalline powder from methanol yielded crystals suitable for X-ray diffraction study.

$L^3NiNa(C_2N_3)$ (5): Addition of NaC_2N_3 (0.09 g, 1×10^{-3} mol) to a stirred solution of $[L^3Ni]{\cdot}1.75H_2O$ (0.46 g, 1×10^{-3} mol) in methanol (20 mL) yielded a dark-green precipitate that was filtered off, washed with methanol, and air dried. Yield: 0.4 g (77%). IR (KBr): $\tilde{\nu}$ = 2932, 2251, 2208, 2144, 1617, 1474, 1448, 1313, 1245, 1233, 1082, 1070, 860, 745, 652, 524, 492 cm^{-1}. UV/Vis: λ = 450 (sh.), 621 nm. $C_{23}H_{24}N_5NaNiO_4$ (516.16): calcd. C 53.5, H 4.7, N 13.6; found C 53.2, H 4.6, N 13.3.

$[L^3NiGd(NO_3)_3(H_2O)_2]$ (6): Compound **6** was prepared as described previously.[9] IR (KBr): $\tilde{\nu}$ = 3513, 3430, 2949, 1644, 1629, 1608, 1476, 1466, 1330, 1294, 1223, 1068, 1030, 928, 852, 746, 738, 644, 482 cm^{-1}. MS (FAB+, 3-nitrobenzyl alcohol matrix): *m*/*z* = 708 (100) $[L^3NiGd(NO_3)_2]^+$. UV/Vis: λ = 442 (sh.), 568, 686 nm.

$(L^3Ni)_2Gd(NO_3)_3(H_2O)_2$ (7): Addition of $[L^3Ni]{\cdot}1.75H_2O$ (0.46 g, 1×10^{-3} mol) to a stirred solution of $L^3NiGd(NO_3)_3(H_2O)_2$ (0.80 g, 1×10^{-3} mol) in acetone yielded a beige precipitate that was filtered off after 30 min. The solid was washed with acetone and air dried. Yield: 0.97 g (78%). Addition of $Gd(NO_3)_3{\cdot}6H_2O$ (0.23 g, 5×10^{-4} mol) to a stirred solution of $L^3Ni{\cdot}2H_2O$ (0.46 g, 1×10^{-3} mol) yielded the same compound. IR (KBr): $\tilde{\nu}$ = 3408, 2954, 1623, 1473, 1450, 1319, 1290, 1245, 1225, 1067, 1028, 974, 855, 740, 645, 482 cm^{-1}. MS (FAB+, 3-nitrobenzyl alcohol matrix): *m*/*z* = 1136 (11) $[(L^3Ni)_2Gd(NO_3)_2]^+$, 1072 (9) $[(L^3Ni)_2Gd(NO_3)]^+$, 708 (100) $[L^3NiGd(NO_3)_2]^+$. UV/Vis: λ = 450 (sh.), 508, 612, 690 nm. $C_{42}H_{52}GdN_7Ni_2O_{19}$ (1233.55): calcd. C 40.9, H 4.2, N 8.0; found C 41.4, H 4.2, N 7.8.

$L^3NiGd(C_2N_3)_2(NO_3)$ (8): Addition of NaC_2N_3 (0.10 g, 1.1×10^{-3} mol) to a stirred solution of $L^3NiGd(NO_3)_3(H_2O)_2$ (0.30 g, 3.7×10^{-4} mol) in methanol (15 mL) yielded a violet precipitate that was filtered off. The solid was washed with methanol and air dried. Yield: 0.28 g (90%). IR (KBr): $\tilde{\nu}$ = 2909, 2306, 2262, 2238, 2189, 2169, 1643, 1632, 1606, 1469, 1291, 1225, 1071, 973, 852, 745, 737, 645, 483 cm^{-1}. MS (FAB+, 3-nitrobenzyl alcohol matrix): *m*/*z* = 712 (100) $[L^3NiGd(N_3C_2)(NO_3)]^+$. UV/Vis: λ = 450 (sh.), 550, 640 nm. $C_{25}H_{24}GdN_9NiO_7$ (778.47): calcd. C 38.6, H 3.1, N 16.2; found C 38.3, H 2.9, N 15.9.

$L^3NiGd(trif)_3(H_2O)_2$ (9): A mixture of $[L^3Ni]{\cdot}1.75H_2O$ (0.23 g, 5×10^{-4} mol) and $Gd(trif)_3$ (0.30 g, 5×10^{-4} mol) in acetone (20 mL) was stirred for 30 min and then filtered. The solution was concentrated to 2–3 mL. Addition of CH_2Cl_2 (15 mL) and stirring at room temperature yielded an off-white precipitate that was filtered and dried. Yield: 0.42 g (79%). IR (KBr): $\tilde{\nu}$ = 3494, 2961, 1631, 1481, 1472, 1435, 1293, 1283, 1234, 1224, 1194, 1169, 1068, 1030, 743, 646, 636, 521 cm^{-1}. MS (FAB+, 3-nitrobenzyl alcohol matrix): *m*/*z* = 882 (100) $[L^3NiGd(trif)_2]^+$. UV/Vis: λ = 438 (sh.), 580, 725 nm. $C_{24}H_{28}F_9GdN_2NiO_{15}S_3$ (1067.62): calcd. C 27.0, H 2.6, N 2.6; found C 26.5, H 2.4, N 2.5.

$(L^3Ni)_2Eu(trif)_3(H_2O)_3$ (10): $[L^3Ni]{\cdot}1.75H_2O$ (0.23 g, 5×10^{-4} mol) and $Eu(trif)_3$ (0.15 g, 2.5×10^{-4} mol) in acetone (15 mL) by using the experimental procedures described above for **9** yielded light-green crystals that were filtered and dried. Yield: 0.23 g (61%). IR (KBr): $\tilde{\nu}$ = 3322, 2957, 1622, 1470, 1438, 1286, 1242, 1220, 1162,

Table 1. Crystallographic data for complexes **2**, **3**, **4**, and **10**.

	2	**3**	**4**	**10**
Formula	$C_{30}H_{38}CuF_9GdN_2O_{16}S_3$	$C_{39}H_{36}Cu_2F_9GdN_4O_{17}S_3$	$C_{42}H_{55}N_4Ni_2O_{11.5}$	$C_{45}H_{54}EuF_9N_4Ni_2O_{20}S_3$
Fw	1169.59	1384.23	917.29	1507.48
Space group	$P\bar{1}$	$C2/c$	$P\bar{1}$	$P2_1/c$
a [Å]	9.173(2)	24.4395(19)	11.204(5)	16.7230(10)
b [Å]	13.747(3)	13.6355(11)	12.097(5)	16.2780(8)
c [Å]	16.855(3)	30.102(2)	16.360(5)	24.1980(5)
α [°]	88.03(3)	90	81.02(3)	90
β [°]	79.80(3)	101.059(6)	85.45(3)	102.802(3)
γ [°]	87.49(3)	90	76.40(3)	90
V [Å^{-3}]	2089.1(7)	9845.0(13)	2126.7(9)	6423.4(5)
Z	2	8	2	4
ρ_{calcd} [g cm^{-3}]	1.859	1.868	1.431	1.559
λ [Å]	0.71073	0.71073	0.71073	0.71073
T [K]	180(2)	100(2)	180(2)	100(2)
μ(Mo-$K_α$) [mm^{-1}]	2.342	2.423	0.951	1.736
R[a] obsd., all	0.0450, 0.0509	0.0506, 0.1078	0.0457, 0.1063	0.1448, 0.2627
R_w[b] obsd., all	0.1065, 0.1099	0.1034, 0.1183	0.0893, 0.1022	0.3336, 0.3935

[a] $R = \Sigma||F_o| - |F_c||/\Sigma|F_o|$. [b] $R_w = [\Sigma w(|F_o^2| - |F_c^2|)^2/\Sigma\, w|F_o^2|^2]^{1/2}$.

1063, 1029, 970, 851, 743, 636 cm^{-1}. MS (FAB+, 3-nitrobenzyl alcohol matrix): *m*/*z* = 1303 (20) $[(L^3Ni)_2Eu(trif)_2]^+$, 1154 (17) $[(L^3Ni)_2Eu(trif)]^+$, 877 (100) $[L^3NiEu(trif)_2]^+$. UV/Vis: *λ* = 632, 936 nm. $C_{45}H_{54}EuF_9N_4Ni_2O_{20}S_3$ (1507.47): calcd. C 35.8, H 3.6, N 3.7; found C 35.8, H 3.5, N 3.6.

Physical Measurements: Elemental analyses were carried out at the Laboratoire de Chimie de Coordination Microanalytical Laboratory in Toulouse, France, for C, H, and N. IR spectra were recorded with a GX system 2000 Perkin–Elmer spectrophotometer; samples were run as KBr pellets. Solid-state (diffuse reflectance) spectra were recorded with a Perkin–Elmer Lambda 35 UV/Vis spectrometer in the 400–1100 nm range. Mass spectra (FAB+) were recorded in dmf as solvent and 3-nitrobenzyl alcohol matrix with a Nermag R10–10 spectrometer. Magnetic data were obtained with a Quantum Design MPMS SQUID susceptometer. All samples were 3-mm diameter pellets molded from ground crystalline samples. Magnetic susceptibility measurements were performed in the 2–300 K temperature range in a 0.1 T applied magnetic field, and diamagnetic corrections were applied by using Pascal's constants.[31] Isothermal magnetization measurements were performed up to 5 T at 2 K. The magnetic susceptibilities were computed by exact calculations of the energy levels associated to the spin Hamiltonian through diagonalization of the full-matrix with a general program for axial symmetry,[32] and with the MAGPACK program package[33] in the case of magnetization. Least-squares fittings were accomplished with an adapted version of the function-minimization program MINUIT.[34]

Crystallographic Data Collection and Structure Determination for 2, 3, 4, and 10: Crystals of **2**, **3**, **4** and **10** (Table 1) were kept in the mother liquor until they were dipped into oil. The chosen crystals were mounted on a Mitegen micromount and quickly cooled down to 180 or 100 K. The selected crystals of **2** (green, 0.37 × 0.16 × 0.12 mm), **3** (light pink, 0.30 × 0.18 × 0.07 mm), **4** (orange, 0.45 × 0.26 × 0.10 mm), and **10** (green) were mounted on a Stoe Imaging Plate Diffractometer System (IPDS) (for **2**, **4**) or an Oxford-Diffraction XCALIBUR (for **3**, **10**) by using a graphite monochromator (*λ* = 0.71073 Å) equipped with an Oxford Cryosystems cooler device. The data were collected at 180 (for **2**, **4**) or 100 K (for **3**, **10**). The unit-cell determination and data integration were carried out by using the CrysAlis RED package for the data recorded with the Xcalibur and the Xred package for the STOE.[35,36] 9369 reflections were collected for **2**, of which 4470 were independent (R_{int} = 0.0672), 36415 reflections for **3**, of which 10056 were independent (R_{int} = 0.0848), 21969 reflections for **4**, of which 12887 were independent (R_{int} = 0.0502), and 45340 reflections for **10**, of which 11730 were independent (R_{int} = 0.3309). The structures were solved by direct methods by using SIR92[37] and refined by means of least-squares procedures on a F^2 with the aid of the program SHELXL97[38] included in the software package WinGX version 1.63.[39] The atomic scattering factors were taken from International Tables for X-ray Crystallography.[40] All hydrogen atoms were geometrically placed and refined by using a riding model. All non-hydrogen atoms were anisotropically refined, and in the last cycles of refinement a weighting scheme was used, where weights were calculated from the following formula: $w = 1/[\sigma^2(F_o^2) + (aP)^2 + bP]$, where $P = (F_o^2 + 2F_c^2)/3$. Although several data sets were recorded on selected crystals of **10**, their poor quality precluded the obtainment of good refinement. Drawings of molecules are performed with the program ORTEP32[41] with 30% probability displacement ellipsoids for non-hydrogen atoms. CCDC-696284 (for **2**), -696285 (for **3**), -696286 (for **4**), and -696287 (for **10**) contain the supplementary crystallographic data for this paper. These data can be obtained free of charge from The Cambridge Crystallographic Data Centre via www.ccdc.cam.ac.uk/data_request/cif.

Supporting Information (see footnote on the first page of this article): Magnetic susceptibility data for complexes **2**, **8**, and **10** in terms of thermal variation of the $\chi_M T$ products.

Acknowledgments

Gh. N. is grateful to NATO for financial support of this work. R. G. is grateful to the European Community for a Marie Curie Fellowship.

[1] a) J.-P. Costes, F. Dahan, A. Dupuis, J.-P. Laurent, *Inorg. Chem.* **1996**, *35*, 2400; b) J.-P. Costes, F. Dahan, A. Dupuis, J.-P. Laurent, *Inorg. Chem.* **1997**, *36*, 3429; c) J. P. Costes, F. Dahan, A. Dupuis, J.-P. Laurent, *Inorg. Chem.* **2000**, *39*, 165.
[2] S. Akine, T. Matsumoto, T. Taniguchi, T. Nabeshima, *Inorg. Chem.* **2005**, *44*, 3270.
[3] C. T. Zeyrek, A. Elmali, Y. Elerman, *J. Mol. Struct.* **2005**, *740*, 47.

[4] A. Bencini, C. Benelli, A. Caneschi, R. L. Carlin, A. Dei, D. Gatteschi, *J. Am. Chem. Soc.* **1985**, *107*, 8128.
[5] R. E. P. Winpenny, *Chem. Soc. Rev.* **1998**, *27*, 447.
[6] M. Sakamoto, K. Manseki, H. Okawa, *Coord. Chem. Rev.* **2001**, *219–221*, 379.
[7] C. Benelli, D. Gatteschi, *Chem. Rev.* **2002**, *102*, 2369.
[8] R. H. Holm, M. J. O'Connor, *Prog. Inorg. Chem.* **1971**, *14*, 241.
[9] J.-P. Costes, F. Dahan, A. Dupuis, J.-P. Laurent, *Inorg. Chem.* **1997**, *36*, 4284.
[10] J.-P. Costes, F. Dahan, J. Garcia-Tojal, *Chem. Eur. J.* **2002**, *8*, 5430.
[11] J.-P. Costes, J. M. Clemente-Juan, F. Dahan, F. Dumestre, J.-P. Tuchagues, *Inorg. Chem.* **2002**, *41*, 2886.
[12] J.-P. Costes, F. Dahan, B. Donnadieu, J. Garcia-Tojal, J. P. Laurent, *Eur. J. Inorg. Chem.* **2001**, 363.
[13] G. Novitchi, S. Shova, A. Caneschi, J.-P. Costes, M. Gdaniec, N. Stanica, *Dalton Trans.* **2004**, 1194.
[14] X.-P. Yang, R. A. Jones, W.-K. Wong, V. Lynch, M. M. Oye, A. L. Holmes, *Chem. Commun.* **2006**, 1836.
[15] W.-K. Wong, X.-P. Yang, R. A. Jones, J. H. Rivers, V. Lynch, W.-K. Lo, D. Xiao, M. M. Oye, A. L. Holmes, *Inorg. Chem.* **2006**, *45*, 4340.
[16] X.-P. Yang, R. A. Jones, Q. Wu, M. M. Oye, W.-K. Lo, W.-K. Wong, A. L. Holmes, *Polyhedron* **2006**, *25*, 271.
[17] J. Paulovic, F. Cimpoesu, M. Ferbinteanu, K. Hirao, *J. Am. Chem. Soc.* **2004**, *126*, 3321.
[18] J. P. Costes, F. Dahan, A. Dupuis, *Inorg. Chem.* **2000**, *39*, 5994.
[19] K. Nakamoto, *Infrared and Raman Spectra of Inorganic and Coordination Compounds*, 5th ed., Wiley, New York, **1997**.
[20] A. B. P. Lever, *Inorganic Electronic Spectroscopy*, Elsevier, **1984**.
[21] A. M. Madalan, N. Avarvari, M. Andruh, *New J. Chem.* **2006**, *30*, 521.
[22] J. H. Van Vleck, A. Frank, *Phys. Rev.* **1929**, *34*, 1494.
[23] G. Novitchi, J.-P. Costes, B. Donnadieu, *Eur. J. Inorg. Chem.* **2004**, 1808.
[24] a) J.-P. Costes, F. Dahan, W. Wernsdorfer, *Inorg. Chem.* **2006**, *45*, 5; b) J. P. Costes, F. Dahan, A. Dupuis, J. P. Laurent, *New J. Chem.* **1998**, *22*, 1525.
[25] T. Yamaguchi, Y. Sunatsuki, M. Kojima, H. Akashi, M. Tsuchimoto, N. Re, S. Osa, N. Matsumoto, *Chem. Commun.* **2004**, 1048.
[26] Q.-Y. Chen, Q.-H. Luo, L.-M. Zheng, Z.-L. Wang, J.-T. Chen, *Inorg. Chem.* **2002**, *41*, 605.
[27] R. Gheorghe, M. Andruh, J. P. Costes, B. Donnadieu, M. Schmidtmann, A. Müller, *Inorg. Chim. Acta* **2007**, *360*, 4044.
[28] T. Shiga, N. Ito, A. Hidaka, H. Okawa, S. Kitagawa, M. Ohba, *Inorg. Chem.* **2007**, *46*, 3492.
[29] C. A. Barta, S. R. Bayly, P. W. Read, B. O. Patrick, R. C. Thompson, C. Orvig, *Inorg. Chem.* **2008**, *47*, 2280.
[30] R. Boca, *Coord. Chem. Rev.* **2004**, *248*, 757.
[31] P. Pascal, *Ann. Chim. Phys.* **1910**, *19*, 5.
[32] A. K. Boudalis, J.-M. Clemente-Juan, F. Dahan, J.-P. Tuchagues, *Inorg. Chem.* **2004**, *43*, 1574.
[33] J. J. Borrás-Almenar, J. M. Clemente-Juan, E. Coronado, B. S. Tsukerblat, *Inorg. Chem.* **1999**, *38*, 6081; J. J. Borrás-Almenar, J. M. Clemente-Juan, E. Coronado, B. S. Tsukerblat, *J. Comput. Chem.* **2001**, *22*, 985.
[34] *MINUIT Program* – A System for Function Minimization and Analysis of the Parameters Errors and Correlations: F. James, M. Roos, *Comput. Phys. Commun.* **1975**, *10*, 345.
[35] *CrysAlis RED*, version 1.170.32, Oxford Diffraction Ltd., **2003**.
[36] *STOE: IPDS Manual*, version 2.75, Stoe & Cie, Darmstadt, Germany, **1996**.
[37] *SIR92: A Program for Crystal Structure Solution*:A. Altomare, G. Cascarano, C. Giacovazzo, A. Guagliardi, *J. Appl. Crystallogr.* **1993**, *26*, 343.
[38] G. M. Sheldrick, *SHELX97* [*Includes SHELXS97*, SHELXL97, CIFTAB]: *Programs for Crystal Structure Analysis*, Release 97–2, Göttingen, Germany, **1998**.
[39] *WINGX – 1.63: Integrated System of Windows Programs for the Solution, Refinement and Analysis of Single Crystal X-ray Diffraction Data*: L. Farrugia, *J. Appl. Crystallogr.* **1999**, *32*, 837.
[40] *International Tables for X-ray crystallography*, Kynoch press, Birmingham, England, **1974**, vol IV.
[41] *ORTEP3 for Windows*: L. J. Farrugia, *J. Appl. Crystallogr.* **1997**, *30*, 565.

Received: July 29, 2008
Published Online: October 21, 2008

